Annals of Biomedical Engineering, Vol. 37, No. 7, July 2009 *(© 2009)* pp. 1464–1473
DOI: 10.1007/s10439-009-9688-z

Cell Death Discrimination with Raman Spectroscopy and Support Vector Machines

GEORGIOS PYRGIOTAKIS,[1] O. ERHUN KUNDAKCIOGLU,[2] KATHRYN FINTON,[1,3] PANOS M. PARDALOS,[2] KEVIN POWERS,[1] and BRIJ M. MOUDGIL[1,4]

[1]Particle Engineering Research Center, University of Florida, Gainesville, FL, USA; [2]Department of Industrial and Systems Engineering, University of Florida, Gainesville, FL, USA; [3]Biochemistry Department, BMSD, University of Washington, Pullman, WA, USA; and [4]Department of Materials Science and Engineering, University of Florida, Gainesville, FL, USA

(Received 19 September 2008; accepted 27 March 2009; published online 14 April 2009)

Abstract—In the present study, Raman spectroscopy is employed to assess the potential toxicity of chemical substances. Having several advantages compared to other traditional methods, Raman spectroscopy is an ideal solution for investigating cells in their natural environment. In the present work, we combine the power of spectral resolution of Raman with one of the most widely used machine learning techniques. Support vector machines (SVMs) are used in the context of classification on a well established database. The database is constructed on three different classes: healthy cells, Triton X-100 (necrotic death), and etoposide (apoptotic death). SVM classifiers successfully assess the potential effect of the test toxins (Triton X-100, etoposide). The cells that are exposed to heat (45 °C) are tested using the classification rules obtained. It is shown that the heat effect results in apoptotic death, which is in agreement with existing literature.

Keywords—Raman spectroscopy, Support vector machines, Death cell discrimination, Toxic chemicals, Cancer treatment.

INTRODUCTION

Cell death and the post-mortem aftermath are integral to the study of many genetic and infectious diseases. It is strongly linked to the toxicological effect of various materials and is of great importance for safe toxicity assessment. In recent literature, cell death is classified in three alternative modes: apoptotic (or type I programmed), autophagic (or type II programmed), and necrotic (or oncotic) cell death. Apoptosis and autophagy are important considerations in the development and treatment of diseases such as cancer,[21–23] and in certain pathogenic infections.[30] Usually apoptosis is marked by caspase activation, chromatin condensation, and the formation of apoptotic bodies. Autophagic is marked by autophagic engulfment of organelles and particles. Cells dying by necrosis display organelle swelling with the eventual loss of plasma, membrane integrity, and subsequent inflammation. Monitoring the cell death process, therefore, is an important step in understanding the pathological processes induced by both disease and pharmaceutical treatments such as anti-cancer drugs.

Despite the importance of this topic, the pathology and biochemical factors and processes adding to cell death are not yet fully understood. Except morphology, *in vivo* there is no single assay that can unambiguously identify cell death type (if such an absolute delineation exists),[18] which makes characterizing cell death even more difficult. A wide range of cytotoxicity assays are presently in use for the determination of cell viability; however, these techniques have shortcomings. They are destructive, time consuming, and expensive. Current assays depend on large populations and cannot measure the health of individual cells. Furthermore, many factors must be considered when interpreting results. Because cytotoxicity assays rely on chemicals and biomarkers, problems may arise due to unwanted interactions during pharmaceutical testing. Furthermore, in the case where assays are dependent upon enzymatic reactions (e.g., MTT, LDH), results may be skewed by promiscuous enzymatic inhibitors. Specificity issues can also lead to complications in the interpretation of results. Kanduc *et al.* compared many of the conventional cytotoxicity assays and find that the reported viability of treated cells differed depending on the assay used.[24] Moreover, a large number of cells is required to determine the exact cellular death and to conclude on the toxicological assessment.

Address correspondence to Panos M. Pardalos, Department of Industrial and Systems Engineering, University of Florida, Gainesville, FL, USA. Electronic mail: gpyrgiotakis@perc.ufl.edu, erhun@ufl.edu, kfinton@gmail.com, pardalos@ufl.edu, kpowers@perc.ufl.edu, bmoudgil@perc.ufl.edu

Raman spectroscopy, a well established analytical tool, is being employed as an alternative for studying cell health. It does not share many of the disadvantages inherent in traditional cytotoxicity assays described above.[33,34] Raman spectroscopy relies on the inelastic scattering of light on matter. It is a complementary technique to the infrared (IR) spectroscopy (FTIR, DRIFT, etc.). The basic difference lies on the polarizability of the molecule that is required by Raman vs. the polarity that is required by traditional IR spectroscopy. In both cases, the material is radiated with a light of specific frequency that induces an electron transition to a different vibrational state, with an energy loss of the photon. In the case of Raman spectroscopy, due to the polarizability of the molecule, the transition occurs through an intermediate state, usually called the *virtual state* (see Fig. 1). The Raman measurements are based on vibrational modes specific to a molecule and its environment. The spectrum of a cell is a representation of its chemical composition and provides an insight for the bio-molecular changes accompanying cellular processes. There are four main advantages for using Raman spectroscopy: (i) the method is noninvasive and does not require chemicals or markers; (ii) measurements can be taken rapidly and in real time, *in vivo*, or *in vitro* without deleterious results to living cells; (iii) it is possible to analyze the health of either a single cell or the entire population; and (iv) the asymmetric nature of water gives a weak Raman signal that, unlike in IR spectroscopy, does not interfere with the spectrum of interest.[50] It has been successfully used to evaluate the toxicity of pharmaceuticals,[36] toxins,[32] and more recently the toxic effect of particles.[41]

While Raman spectroscopy has many advantages, there exists one large drawback; highly complex spectra. Because the spectrum of a cell contains information from all cellular components, detecting minute

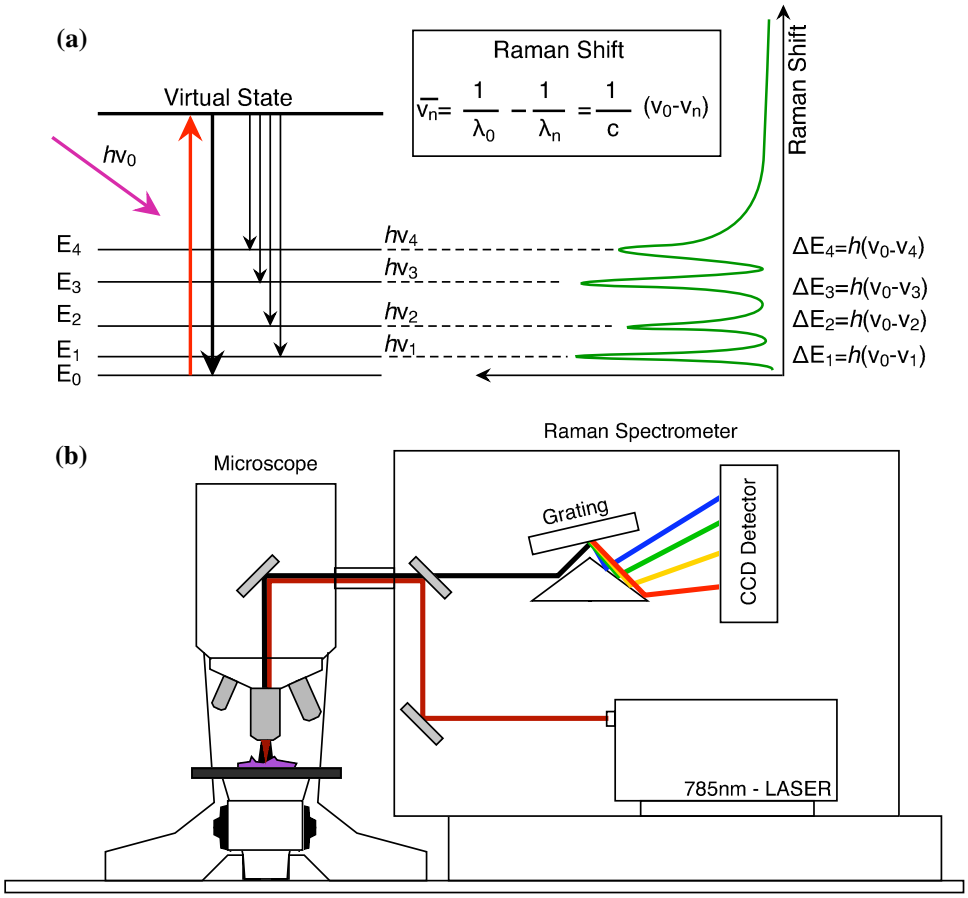

FIGURE 1. The basic principles of Raman spectroscopy. (a) A photon of a certain energy and frequency induces vibrational transitions on the examined molecule, by giving a portion of its energy. The transition occurs through a virtual state, created due to the polarizability of the studied molecule. The scattered photon has lower energy than the incident and the energy difference in between is measured by the detector. This is referred to as the *Raman Shift*. (b) The micro Raman utilizes a microscope and focuses the laser through the objective lens on the sample. The scattered photons are collected by the same objective lens and travel the Raman spectrometer, where they are analyzed by a grating and a CCD detector.

changes from one spectrum to the next can be a daunting task. Traditionally, peak fitting has been used to analyze Raman (and FTIR) spectra. Peak fitting relies on the recognition of peaks representing certain cellular components and correlating their relative peak intensities to their biochemical concentrations within the cell. The relative changes in peak intensity over time are in direct response to the changing biochemical and biophysical factors that are related to the health viability, and eventually to the cell death type and process. However, due to the large number of overlapping peaks, this task becomes very tedious and time consuming. The traditional methodology for analyzing the spectra includes an elaborate series of algorithms. A series of spectra is obtained (see Fig. 2a) and a series of mathematical procedures is followed to remove the baseline, the fluorescence, to normalize the spectra, and to calculate the average and the standard deviation (see Fig. 2b). Furthermore, the analysis depends on the presumption that one already knows which peaks are discriminant, and those peaks must be prevalent spectral features with limited interference from background noise and overlapping peaks. Thus, it is critical to develop a method that is applicable for high throughput screening, is simpler than peak fitting to execute, and utilizes the entire spectrum instead of predetermined sections. Moreover, an automated method is desired that can derive results without any manual spectra processing.

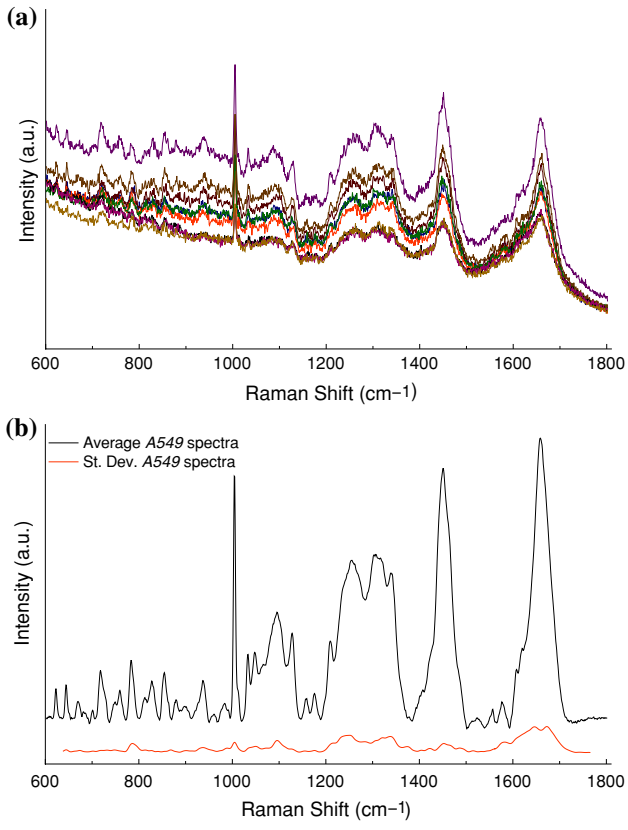

FIGURE 2. (a) Spectra acquired from 10 different cells after 24 h on MgF_2 crystal. (b) The average spectrum and standard deviation of 30 A549 cells spectra, after 24 h on the MgF_2.

For such scientific experiments that generate a large number of measurements and features in each measurement, *machine learning techniques* can be used to analyze the data and derive conclusions. *Supervised learning* refers to the capability of a system to learn from a set of examples, which is a set of input/output pairs. The input is usually a *vector of features* for an object, and the output is the *label* for the class this object belongs to. A set of objects with feature vectors and corresponding class labels is called a *training set*. This set can be used to derive classification or regression functions. The trained system is capable of predicting the label of an object. The term *supervised* originates from the fact that the labels for the objects, which are provided as input in the training set, have to be determined by an outside source. This outside source is usually referred to as the *supervisor*. In this study, cells are labeled as control or death depending on the type of the drug used. Next, classification functions are derived to validate the model and test the labels for cells that are subject to abnormal heat.

The remainder of the paper is organized as follows: section "Methods" presents the methods used and the details for the experiments. Computational results are presented in section "Results and Discussion." The last section gives concluding remarks and directions for future research.

METHODS

Cell Culture protocols

For this set of experiments the A549 lung epithelia cells are used (from ATCC; cell line number CCL-185). This is a hypo-triploid human cell line with the modal chromosome number 12, occurring in 24% of cells. The line is initiated in 1972 by Giard *et al.* through explants culture of lung carcinomatous tissue from a 58-year-old Caucasian male.[12]

The growth media is made by 89% RPMI-1640 with L-glutamine (from Cellgro; Cat #: 25-053-CI), 10% fetal bovine serum (four times filtered through 0.1-μm filter, from Hyclone; Cat. #: SH30070.03), and 1% antibiotic-antimycotic solution (from Cellgro; Cat. #: 30-004-CL). The cells are grown with complete growth media in a 25-cm^2 cell culture flask at 37 °C, and 5% CO_2. In order to harvest the cells for various experimental applications, the culture medium is removed and the cells are rinsed with 1× Hank's balanced salt solution (HBSS) without Ca^{2+} or Mg^{2+} (from ATCC;

Cat. #: 30-22/3) to remove all traces of serum that contains trypsin inhibitor. One mL of 0.25% Trypsin/2.21 mM EDTA in HBSS without sodium bicarbonate, calcium, and magnesium (from Cellgro; Cat. #: 25-053-CL) is added to the flask and the cells are observed under an inverted microscope until cell layer is detached (usually within 2–5 min). Occasionally gentle agitation is required to achieve the cell removal in reasonable time frame, since long exposure to the trypsin can damage the cells. Five mL of complete growth medium is added to deactivate the trypsin, and the cell suspension is centrifuged for 3 min at 1000 rpm. The supernatant is removed and 1 mL of fresh complete media is added, and the cells are gently aspirated resulting into a homogeneous solution of ~3×10^6 cells/mL and viability ration above 95%. The cell count is done with the ViCell from Beckmann-Coulter (Fullerton, CA). This solution is used for seeding with proximately ~5×10^3 cells on a 5×5 mm^2 MgF_2 substrate (custom made by Red-Optronics) used in the Raman. The MgF_2 crystal is used to reduce the background radiation from the petri-dish. The seeded MgF_2 substrates are placed in a 6-well plate (9.6 cm^2 per well) in the incubator for 45 min, sufficient for the cells to attach onto the MgF_2. Three mL of growth media is added and the seeded cells are incubated at 37 °C and 5% CO_2 for a minimum of 24 h before the toxin dosing.

Toxic Agent Dosing

After reaching 80% confluency (on the MgF_2 plate) the growth media is removed and the cells are rinsed twice with HBSS to remove traces of proteins. Following this, the cells are rinsed with the full media twice to ensure that possible traces of HBSS will not be significant to alter the final concentration of growth media. Finally, 2 mL of media containing the toxic agent are added and the cells are moved in the incubator. Prior to each experiment, the media is removed and the cells are rinsed with HBSS twice and fresh RPMI 1640 is used since the media proteins can interfere with the obtained spectrum. The absence of proteins does not have any effect on the cells for the time period the experiments last (approximately 1 h).[54] The RPMI 1640 provides all the necessary growth hormones and sugars essential for the cell viability.

Toxic Agents Standards

The triggers for the two different cellular deaths are etoposide (apoptosis) and Triton X-100 (necrosis). Etoposide is a strong chemotherapeutic drug, used as a form of chemotherapy for malignancies such as Ewing's sarcoma, lung cancer, testicular cancer, lymphoma, nonlymphocytic leukemia, and glioblastoma multiforme. Etoposide is known to form a ternary complex with DNA and topoisomerase II causing double-stranded DNA breaks which is one of the defined mechanisms for the apoptosis.[25] It has also been shown to upregulate p53, an initiator of apoptosis.[17,46] Triton X-100 is used as a benchmark in various assays, since it can rapture the cellular membrane and results in the necrotic death of the cells. Triton X-100 exposure is reported to increase the expression of apoptosis inhibitors and is known to solubilize and destabilize the cell membrane.[5]

The toxin concentrations are selected based on the literature that suggest that these values will impact the cells, but not catastrophically. For the experiments, the agents concentration is 100 μM for Triton-X[33] and 80 μM,[25,36,53] for the etoposide. These concentrations are expected to induce damage in the cells without completely lysing the cells in the first 24 h of the experiment. The solution is prepared immediately prior to dosing. The etoposide is insoluble in water, so a stock solution is prepared with 100 mM of etoposide in di-methyl-sulfo-oxide (DMSO).

Raman Spectroscopy Protocols and Procedures

The Raman microscope used is the InVia system by Renishaw, consisting of a Leica microscope connected to a Renishaw 2000 spectrometer. The high power diode laser (250 mW) produces laser light of 785 nm and does not cause any damage to the cells even after 40 min exposure time. The MgF_2 plate after rinsing with the HBSS is moved on a Delta T Culture Dish (from Biotechs; Cat #: 04200415C), and 2 mL of RPMI 1640 is added. The dish is placed onto a heating stage (Delta T4 Culture Dish Controller, Biotechs, Butler, PA) to maintain 37 °C through the entire measurement and induce the required heating. The laser is focused over the center of the cell, with the help of the crosshair, through the Leica microscope. The spot size is 20×40 μm^2 when focused on dry Si wafer and 20×30 μm^2 when in water based liquid. It can be assumed therefore that the laser spot can cover the whole cell (20×20 μm^2 when 80% confluent, 40×40 μm^2 when isolated). Although the laser spot can be larger than the cell, since the intensity of the laser follows a Gaussian distribution around the geometric center, the parts that are not from the measured cell, are not contributing significantly. However, for the isolated cells the relative position of the laser can potentially effect the spectrum and therefore they are not included in this study. The 785-nm laser beam passes through the 63× water immersion Leica objective and the final output power is 48 mW. In this study, we collect spectra from cells adhered onto MgF_2 plate.

The MgF_2 plate is used to eliminate the background signal from the petri dish. The collection time for each spectrum is set to 30 s. However, the instrument requires an additional 70 s to read the detector, during which the cell is exposed to the laser. Therefore, the total exposure time is 100 s and immediately after the measurement is preformed, the laser shutter is turned off, a new cell is selected, and the following measurement is immediately executed.

The RPMI media with or without the presence of the various toxins does not influence the spectra. In previous publications, we have developed an algorithm that takes the background, the fluorescence, and the normalization of the spectra into account.[3,29] In the present work, the background is obtained and subtracted from the spectra following nonlinear subtraction.[29] The spectrum before and after are used for classification, but there is no significant difference in the final results. Therefore we omit this step since it is likely that these processes hinder or remove information, essential for the classification techniques.

Support Vector Machines

Developed by Vapnik,[48] support vector machines (SVMs) are the state-of-the-art supervised machine learning methods. SVM classifiers classify two linearly separable sets of pattern vectors that belong to two different classes. The classification function is defined by a hyperplane. Although there are infinitely many hyperplanes that separate the two classes, SVM classifiers find the hyperplane that maximizes the distance from the convex hulls of both classes by solving a quadratic convex optimization problem. The success and robustness of SVM classifiers rely on strong fundamentals from the statistical learning theory, from which generalization bounds are derived. SVMs can be extended to nonlinear classification by implicitly embedding the original data in a nonlinear space using *kernel functions*.[45]

SVMs have a wide spectrum of application areas such as pattern recognition,[28] text categorization,[19] biomedicine,[6,7,31,37,44] brain–computer interface,[10,27] and finance.[16,47] The training is performed by minimizing a quadratic convex function that is subject to linear constraints. Quadratic programming (QP) is an extensively studied field of optimization theory and there are many general purpose methods to solve QP problems such as quasi-Newton, primal-dual, and interior-point methods.[2] These general purpose methods are suitable for small size problems. In order to solve large problems, faster methods are required. For SVM classifiers, these faster methods involve chunking[35] and decomposition[39] techniques, which use subsets of points to find the optimal hyperplane. SVM Light[20] and LIBSVM[15] are among the most frequently used software applications that use chunking and decomposition methods efficiently.

Next, we give a brief introduction to the mathematical aspects of SVM classifiers. Let $\mathbf{x}_i \in \mathbb{R}^d$ be a set of pattern vectors, with class labels $y_i \in \{1, -1\}$ for $i = 1, \ldots, n$. The problem of classifying these pattern vectors consists of finding a function $f(\cdot)$ which correctly assigns a class label for a given pattern vector $\mathbf{x}$. Assume that the pattern vectors in the positive and negative classes are to be separated by a hyperplane $\langle \mathbf{w} \cdot \mathbf{x}_i \rangle + b = 0$ which is represented as the vector $\mathbf{w}$ and the offset parameter b. Let the distance between the hyperplane and the closest pattern vector $\mathbf{x}^*$ be $|(\langle \mathbf{w} \cdot \mathbf{x}^* \rangle) + b|$, which is called the *functional margin*. Note that the goal is to maximize the *geometric margin*, which is obtained by dividing the functional margin by the norm of the hyperplane, $\|\mathbf{w}\|$. Setting the functional margin to 1 for the closest pattern vectors in positive and negative classes, the separating hyperplane with the maximum geometric margin is obtained by maximizing the reciprocal of $\|\mathbf{w}\|$. This is equivalent to minimizing $\|\mathbf{w}\|$ which can be rewritten as

$$\begin{aligned} \min_{\mathbf{w},b,\xi} \quad & \tfrac{1}{2}\|\mathbf{w}\|^2 + \tfrac{C}{2}\sum_{i=1}^{n} \xi_i^2 \\ \text{subject to} \quad & y_i(\langle \mathbf{w} \cdot \mathbf{x}_i \rangle + b) \geq 1 - \xi_i \qquad i = 1, \ldots, n \end{aligned} \tag{1}$$

where ξ are the slack variables for misclassified pattern vectors and C is the penalty term in the objective function for such vectors. The role of scalar C is to control the trade-off between margin violation and regularization. This formulation can be converted into a nonlinear classification method by taking its Lagrangian dual and implementing kernel methods.[8,49]

The Lagrangian dual problem for (1) can be written as

$$\begin{aligned} \max_{\alpha} \quad & \sum_{i=1}^{n} \alpha_i - \tfrac{1}{2C}\sum_{i=1}^{n} \alpha_i^2 - \tfrac{1}{2}\sum_{i=1}^{n}\sum_{j=1}^{n} y_i y_j \alpha_i \alpha_j \langle \mathbf{x}_i \cdot \mathbf{x}_j \rangle \\ \text{subject to} \quad & \sum_{i=1}^{n} y_i \alpha_i = 0 \\ & \alpha_i \geq 0 \qquad i = 1, \ldots, n. \end{aligned} \tag{2}$$

In formulation (2), the pattern vectors appear only in the form of dot products and nonlinear maps can be used to embed them in a higher dimensional space. Then the separation can be done on the mapped pattern vectors in this higher dimensional space. The embedding is done via the *kernel trick* and the mapping is defined over dot product *Hilbert* spaces. This transformation replaces the dot product $\langle \mathbf{x}_i \cdot \mathbf{x}_j \rangle$, with a nonlinear kernel $K(\mathbf{x}_i, \mathbf{x}_j)$. Kernel functions are sometimes referred to as *Mercer kernels*, because they must satisfy Mercer's condition.[38]

The experimental procedure starts by constructing a basic 56 × 1301 matrix based on the two classes the data must be discriminated to. The discrimination is done always among two different classes. The 56 columns consist of 25 from class 1, 25 from class 2, 3 test subjects from class 1, and 3 test subjects from class 2. The rows represent the different frequencies (600–1800 cm^{-1} with step 0.92 cm^{-1}), while the columns are spectra of different cells in different environmental conditions. There are three different matrices studied; *Necrotic* (NC): Triton X-100 and Control, *Apoptotic* (AC): Etoposide and Control, and *Necrotic vs. Apoptotic* (NA): Triton X-100 and Etoposide. For the validation of classification algorithm, in addition to the 50 data instances of the library, we use three control cells and seven cells with toxins.

To represent the results, we plot the points with x-axis to be the sample ID and y-axis the distance from the hyperplane that separates the two classes. SVM[20] is used to train the data in this study. Linear classifiers are used and the trade-off parameter C is set after leave-one-out cross validation technique is employed. When using the leave-one-out method, SVM is trained multiple times, using all but one of the instances in the training set that is selected randomly. The highest prediction accuracy is achieved for $C = 1000$ for training sets of all experiments. Therefore, we set parameter C to 1000 in our computational studies.

RESULTS AND DISCUSSION

Triton X-100- and Etoposide-Induced Cellular Death Discrimination

Although the data used for supervised classification are Triton X-100, etoposide, and healthy cells, the first test to validate the accuracy of the classification algorithms is to attempt to classify same type of data (self-validating). For these experiments a series of new spectra is obtained under the same conditions as described above. The concentration of the toxins are kept the same and the exposure time is 24 h 30 spectra are obtained from each case (Triton X-100 and etoposide) and randomly seven are selected to evaluate the algorithm. In addition, parallel with every toxin measurement, a control cell experiment is conducted to further validate the model. From that data set, three spectra are randomly selected to even the number of unknowns to 10.

Ideally, the data is expected to have a functional margin of at least 1. However, since the cells are not from the same passage and there are other conditions (humidity, small alterations at the full growth media) that can induce variations, it is not always possible to keep the distance more than 1 (or less than −1). Furthermore, the interaction of each cell individually with the toxin is not the same, due to the complexity of its nature. As it can be seen in Figs. 3a and 3b, SVM classifiers successfully discriminate the control cells from etoposide and Triton X-100, respectively. The distance from the separating hyperplane and small variation showcase the classification and prove the ability of the algorithm to classify the obtained spectra in two classes.

Case Study: Heat-Induced Cellular Death

For the past four decades hyperthermia has been used to potentiate the cytotoxic effects of ionizing radiation[11,42] and chemotherapy.[14,42] It has been established that elevated temperatures alone cause cell death in a predictable manner that is linearly

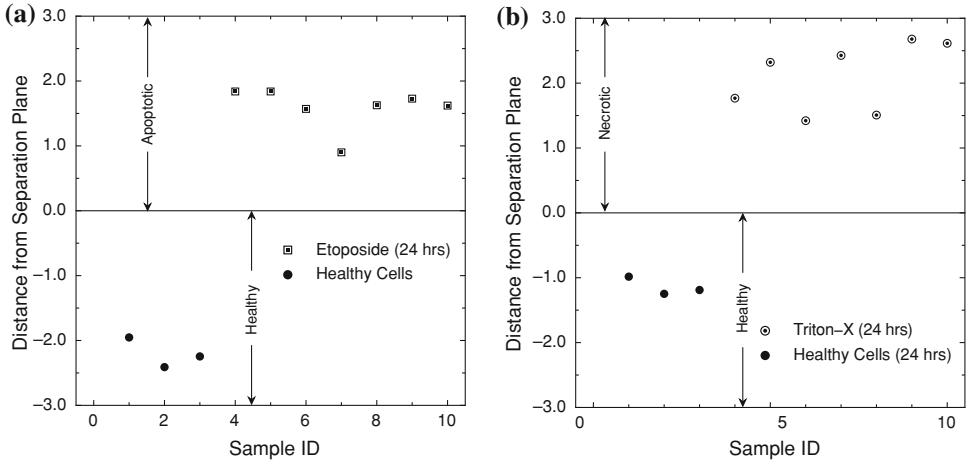

FIGURE 3. Demonstration of the pattern recognition based on SVM classification. (a) The classification of the etoposide-induced apoptotic death after 24 h exposure. (b) The Triton X-100-induced apoptosis on the MgF_2.

dependent on exposure time and is nonlinearly dependent on temperature.[9,43] A variety of cell lines, including A549, have been reported to undergo apoptosis[1,13] during mild heat treatment and necrosis during prolonged or intensified exposure.[14,26,40] In this study, heat treatment at 45 °C over 30 min is used to test the predictive strength of the model by using a different cell death trigger that would induce a form of programmed cell death. The heating stage Delta T4 Culture Dish Controller is used and the ramping rate is approximately 0.5 °C/min. The spectra are obtained after 30 min of exposure to the heat. As in the previous case, in parallel to this experiment, control, apoptotic (etoposide), and necrotic (Triton X-100) cells are used after 24 h exposure.

Assuming that the effect of the heat is the unknown sample, we try to attempt classification, among all the three classes, *healthy*, *apoptotic*, and *necrotic*. Since there are many drawbacks of hyperplane-based multiclass learning techniques,[4] pairwise examination is performed across all the possible combinations. So in this particular case we examine, Healthy–Necrotic, Healthy–Apoptotic, and Apoptotic–Necrotic. In Fig. 4a are the results of the heating experiment as it is attempted for apoptotic death vs. healthy cells. The heating experiment is classified as apoptotic death. As it can be seen in the figure, most of the samples are lying between 0.3 and 1.0 in regards to the distance from the hyperplane. The next step is to check the case of the necrotic cell death vs. healthy cells. In this case, the results of the classification appear to be scattered among both classes, while the test instances are classified correctly (see Fig. 4b). This is an inconclusive result since there is no particular trend. This can happen, either because the classification is wrong, or because some of the instances are indeed necrotic. If the second is true, then a classification among apoptotic vs. necrotic will classify them again as necrotic. Therefore, the last classification is performed among the necrotic and apoptotic cells. Figure 4c shows that all the heating spectra are classified again as apoptotic. So in the cases where the apoptotic death is used as one

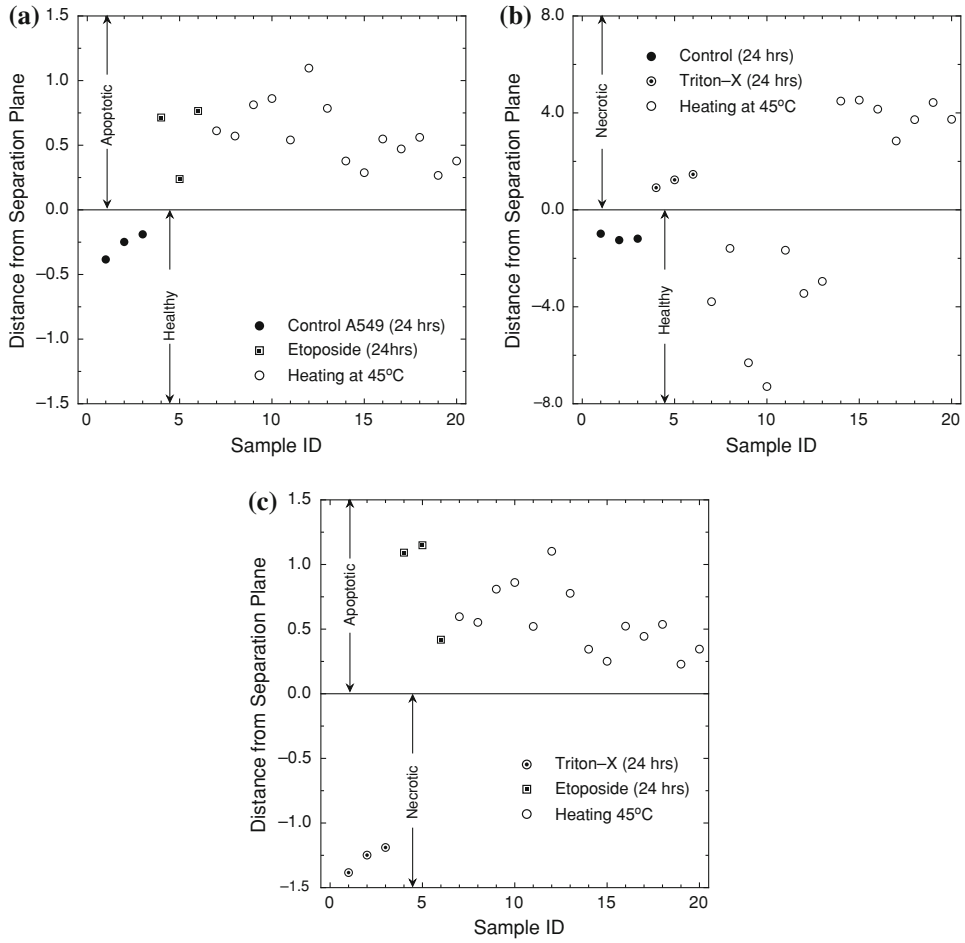

FIGURE 4. The classification of the heating effect. (a) The heating in comparison with the healthy and the apoptotic, (b) the heating in comparison with the healthy and the necrotic, and (c) the heating in comparison to the necrotic and the apoptotic.

of the two classes, the heat exposed cells are classified as apoptotic.

CONCLUDING REMARKS

The coupling of Raman spectroscopy, a very powerful and noninvasive technique, with SVM classification algorithms is used to identify cellular death induced by toxins and by low temperature heating. Although there are very few known reports[51,52] that combine these two fields, it is the first known attempt toward the issue of cell death identification. The classification models built with Raman spectral data can be used to discriminate between minute biochemical differences within cells rapidly, in real time, and in a nondestructive and noninvasive manner. A very important aspect, further highlighting the results, is the success to classify biological samples that can present alteration, and differences in their signal due to external (or internal) parameters. Those alterations are manifested to the current project by the variations in the distance from the separating hyperplane. Cases, however, in real biological systems always exhibit minute variations and alteration. The success of this technique (Raman-SVM) is showcased by the fact that although it is able to detect these minute changes, it does not prevent the algorithm from correctly classifying the results.

This study sets the foundation for developing diagnostic tools for cancer or other genetic diseases, the cellular response to chemotherapy, and the toxicity assessment of drugs and particles. Future work will explore the sensitivity of this technique in terms of its ability to distinguish finer biochemical or biophysical processes related to cell death such as caspase activation or chromatin condensation. It is critical to expand this methodology to include more than two classes without pairwise comparison and therefore being able to distinguish immediately between various stages of the cell.

ACKNOWLEDGMENTS

The authors are grateful for useful comments from two anonymous referees. The authors also acknowledge the financial support of the Particle Engineering Research Center (PERC) at the University of Florida, the State of Florida, the National Science Foundation (NSF Grant EEC-94-02989, NSF-NIRT Grant EEC-0506560, National High Field Magnet Laboratory), the National Institutes of Health (Grants 1-P20-RR020654-01, RO1HL75258, R01HL78670), and the Industrial Partners of the PERC for support of this research. Any opinions, findings, and conclusions or recommendations expressed in this material are those of the author(s) and do not necessarily reflect those of the National Science Foundation. Research of Panos M. Pardalos is partially supported by NSF and Air Force grants.

REFERENCES

[1]Armour, E. P., D. McEachern, Z. Wang, P. M. Corry, and A. Martinez. Sensitivity of human cells to mild hyperthermia. *Cancer Res.* 53(12):2740–2744, 1993.

[2]Bennet, K., and C. Campbell. Support vector machines: Hype or hallelujah? *SIGKDD Explor.* 2(2):1–13, 2000.

[3]Bhowmick, T. K., G. Pyrgiotakis, K. Finton, A. K. Suresh, S. G. Kane, J. R. Bellare, and B. M. Moudgil. A study of the effect of JB particles on *Saccharomyces cerevisiae* (yeast) cells by Raman spectroscopy. *J. Raman Spectrosc.* 39(12):1859–1868, 2009. doi:10.1002/jrs.2051.

[4]Bishop, C. M. Pattern Recognition and Machine Learning (Information Science and Statistics). Berlin: Springer, 2006.

[5]Boesewetter, D., J. Collier, A. Kim, and M. Riley. Alterations of a549 lung cell gene expression in response to biochemical toxins. *Cell Biol. Toxicol.* 22(2):101–108, 2006.

[6]Brown, M., W. Grundy, D. Lin, N. Cristianini, C. Sugne, T. Furey, M. Ares, and D. Haussler. Knowledge-based analysis of microarray gene expression data by using support vector machines. *Proc. Natl. Acad. Sci. USA* 97(1): 262–267, 2000.

[7]Cifarelli, C., and G. Patrizi. Solving large protein folding problem by a linear complementarity algorithm with 0-1 variables. *Optim. Methods Softw.* 22(1):25–49, 2007.

[8]Cristianini, N., and J. Shawe-Taylor. An Introduction to Support Vector Machines. Cambridge: Cambridge University Press, 2000.

[9]Dewhirst, M. W., D. A. Sim, S. Sapareto, and W. G. Connor. Importance of minimum tumor temperature in determining early and long-term responses of spontaneous canine and feline tumors to heat and radiation. *Cancer Res.* 44(1):43–50, 1984.

[10]Garcia, G. N., T. Ebrahimi, and J. M. Vesin. Joint time-frequency-space classification of EEG in a brain-computer interface application. *J. Appl. Signal Process.* 7:713–729, 2003.

[11]Gerner, E. W., W. G. Connor, M. L. Boone, J. D. Doss, E. G. Mayer, and R. C. Miller. The potential of localized heating as a adjunct to radiation therapy. *Radiology* 116(02):433–439, 1975.

[12]Giard, D. J., S. A. Aaronson, G. J. Todaro, P. Arnstein, J. H. Kersey, H. Dosik, and W. P. Parks. In vitro cultivation of human tumors: Establishment of cell lines derived from a series of solid tumors. *J. Natl. Cancer Inst.* 51(5):1417, 1973.

[13]Hayashi, S., M. Hatashita, H. Matsumoto, Z. H. Jin, H. Shioura, and E. Kano. Modification of thermosensitivity by amrubicin or amrubicinol in human lung adenocarcinoma a549 cells and the kinetics of apoptosis and necrosis induction. *Int. J. Mol. Med.* 16:381–387, 2005.

[14]Hildebrandt, B., P. Wust, O. Ahlers, A. Dieing, G. Sreenivasa, T. Kerner, R. Felix, and H. Riess. The cellular and molecular basis of hyperthermia. *Crit. Rev. Oncol. Hematol.* 43(1):33–56, 2002.
[15]Hsu, C. W., C. C. Chang, and C .J. Lin. A practical guide to support vector classification. http://www.csie.ntu.edu.tw/~cjlin/papers/guide/guide.pdf, 2004.
[16]Huang, Z., H. Chen, C. J. Hsu, W. H. Chen, and S. Wuc. Credit rating analysis with support vector machines and neural networks: A market comparative study. *Decis. Support Syst.* 37:543–558, 2004.
[17]Huang, P., and W. Plunkett. A quantitative assay for fragmented DNA in apoptotic cells. *Anal. Biochem.* 207(1): 163–167, 1992.
[18]Jaeschke, H., J. S. Gujral, and M. L. Bajt. Apoptosis and necrosis in liver disease. *Liver Int.* 24(2):85–89, 2004.
[19]Joachims, T. Text categorization with support vector machines: Learning with many relevant features. In: Proceedings of the European Conference on Machine Learning, edited by C. Nédellec and C. Rouveirolpages. Berlin: Springer, 1998, pp. 137–142.
[20]Joachims, T. Making large–scale SVM learning practical. In: Advances in Kernel Methods: Support Vector Learning, edited by B. Schölkopf, C. J. C. Burges, and A. J. Smola. Cambridge, MA: MIT Press, 1999, pp. 169–184.
[21]Kanduc, D., P. Bannasch, and E. Farber. A critical perspective in cancer research (review). *Int. J. Oncol.* 15(6): 1213–1220, 1999.
[22]Kanduc, D., F. Capuano, S.A. Capurso, J. Geliebter, D. Guercia, A. Lucchese, A. Mittelman, S. M. Simone, A. A. Sinha, R. Tiwari, and E. Farber. Cancer prevention and therapy: Strategies and problems. *J. Exp. Ther. Oncol.* 3(3):108–114, 2003.
[23]Kanduc, D., J. Geliebter, A. Lucchese, R. Mazzanti, A. Mittelman, L. Polimeno, A. Ponzetto, R. Santacroce, S. Simone, E. Sinigaglia, A. A. Sinha, L. Tessitore, R. K. Tiwari, and E. Farber. Gene therapy in cancer: The missing point. *J. Exp. Ther. Oncol.* 5(2):151–158, 2005.
[24]Kanduc, D., A. Mittelman, R. Serpico, E. Sinigaglia, A. A. Sinha, C. Natale, R. Santacroce, M. G. Di Corcia, A. Lucchese, L. Dini, P. Pani, S. Santacroce, S. Simone, R. Bucci, and E. Farber. Cell death: Apoptosis versus necrosis (review). *Int. J. Oncol.* 21(1):165–170, 2002.
[25]Karpinich, N. O., M. Tafani, R. J. Rothman, M. A. Russo, and J. L. Farber. The course of etoposide-induced apoptosis from damage to DNA and p53 activation to mitochondrial release of cytochrome c. *J. Biol. Chem.* 277(19): 16547–16552, 2002.
[26]Komata, T., T. Kanzawa, N. Takeo, A. Hiroshi, S. Endo, M. Nameta, T. Hideaki, Y. Tadashi, K. Seiji, and T. Ryuichi. Mild heat shock induces autophagic growth arrest, but not apoptosis in u251-mg and u87-mg human malignant glioma cells. *J. Neuro-Oncol.* 68:101–111, 2004.
[27]Lal, T. N., M. Schroeder, T. Hinterberger, J. Weston, M. Bogdan, N. Birbaumer, and B. Schölkopf. Support vector channel selection in BCI. *IEEE Trans. Biomed. Eng.* 51(6):1003–1010, 2004.
[28]Lee, S., and A. Verri. Pattern recognition with support vector machines. In: SVM 2002, Niagara Falls, Canada. Berlin: Springer, 2002.
[29]Maquelin, K., L. P. Choo-Smith, T. van Vreeswijk, H. P. Endtz, B. Smith, R. Bennett, H. A. Bruining, and G. J. Puppels. Raman spectroscopic method for identification of clinically relevant microorganisms growing on solid culture medium. *Anal. Chem.* 72(1):12–19, 2000.
[30]Navarre, W. W., and A. Zychlinsky. Pathogen-induced apoptosis of macrophages: A common end for different pathogenic strategies. *Cell. Microbiol.* 2(4):265–273, 2000.
[31]Noble, W. S. Support vector machine applications in computational biology. In: Kernel Methods in Computational Biology, edited by B. Schoelkopf, K. Tsuda, and J.-P. Vert. Cambridge, MA: MIT Press, 2004, pp. 71–92.
[32]Notingher, I., C. Green, C. Dyer, E. Perkins, N. Hopkins, C. Lindsay, and L. L. Hench. Discrimination between ricin and sulphur mustard toxicity in vitro using Raman spectroscopy. *J. R. Soc. Interface* 1(1):79–90, 2004.
[33]Notingher, I., S. Verrier, S. Haque, J. M. Polak, and L. L. Hench. Spectroscopic study of human lung epithelial cells (a549) in culture: Living cells versus dead cells. *Biopolymers* 72(4):230–240, 2003.
[34]Notingher, I., S. Verrier, H. Romanska, A. E. Bishop, J. M. Polak, and L. L. Hench. In situ characterisation of living cells by Raman spectroscopy. *Spectrosc. Int. J.* 16(2):43–51, 2002.
[35]Osuna, R. F. E., and F. Girosi. An improved training algorithm for support vector machines. In: IEEE Workshop on Neural Networks for Signal Processing, Amelia Island, FL, 1997, pp. 276–285.
[36]Owen, C. A., J. Selvakumaran, I. Notingher, G. Jell, L. L. Hench, and M. M. Stevens. In vitro toxicology evaluation of pharmaceuticals using Raman micro-spectroscopy. *J. Cell. Biochem.* 99(1):178–186, 2006.
[37]Pardalos, P. M., V. L. Boginski, and A. Vazacopoulos, editors. Data Mining in Biomedicine. Berlin: Springer, 2007.
[38]Pardalos, P. M., and P. Hansen, editors. Data Mining and Mathematical Programming. Providence, RI: American Mathematical Society, 2008.
[39]Platt, J. Fast training of SVMs using sequential minimal optimization. In: Advances in Kernel Methods: Support Vector Learning, edited by B. Schölkopf, C. J. C. Burges, and A. J. Smola. Cambridge, MA: MIT Press, 1999, pp. 185–208.
[40]Prasad, K. V., A. Taiyab, D. Jyothi, U. K. Srinivas, and A. S. Sreedhar. Heat shock transcription factors regulate heat induced cell death in a rat histiocytoma. *J. Biosci.* 32(3):585–593, 2007.
[41]Pyrgiotakis, G., T. K. Bhowmick, K. Finton, A. K. Suresh, S. G. Kane, J. R. Bellare, and B. M. Moudgil. Cell (a549)-particle (Jasada Bhasma) interactions using Raman spectroscopy. *Biopolymers* 89(6):555–564, 2008.
[42]Robinson, J. E., M. J. Wizenberg, and W. A. McCready. Combined hyperthermia and radiation suggest and alternative to heavy particle therapy for reduced oxygen enhancement ratios. *Nature* 251(5475):521–522, 1974.
[43]Sapareto, S. A., and W. C. Dewey. Thermal dose determination in cancer therapy. *Int. J. Radiat. Oncol. Biol. Phys.* 10(6):787–800, 1984.
[44]Seref, O., O. E. Kundakcioglu, and P. M. Pardalos, editors. Data Mining, Systems Analysis and Optimization in Biomedicine, vol. 953. Melville, NY: American Institute of Physics, 2008.
[45]Shawe-Taylor, J., and N. Cristianini. Kernel Methods for Pattern Analysis. Cambridge: Cambridge University Press, 2004.
[46]Solovyan, V., Z. Bezvenyuk, V. Huotari, T. Tapiola, T. Suuronen, and A. Salminen. Distinct mode of apoptosis induced by genotoxic agent etoposide and serum withdrawal in neuroblastoma cells. *Brain Res. Mol. Brain Res.* 62(1):43–55, 1998.

[47]Trafalis, T. B., and H. Ince. Support vector machine for regression and applications to financial forecasting. In: International Joint Conference on Neural Networks (IJCNN'02), Como, Italy, 2002.
[48]Vapnik, V. The Nature of Statistical Learning Theory. Berlin: Springer-Verlag, 1995.
[49]Vapnik, V. Statistical Learning Theory. New York: Wiley, 1998.
[50]Verrier, S., I. Notingher, J. M. Polak, and L. L. Hench. In situ monitoring of cell death using Raman microspectroscopy. *Biopolymers* 74(1–2):157–162, 2004.
[51]Widjaja, E., G. H. Lim, and A. An. A novel method for human gender classification using Raman spectroscopy of fingernail clippings. *Analyst* 133:493–498, 2008.
[52]Widjaja, E., W. Zheng, and Z. Huang. Classification of colonic tissues using near-infrared Raman spectroscopy and support vector machines. *Int. J. Oncol.* 32(3):653–662, 2008.
[53]Yogalingam, G., and A. M. Pendergast. Serum withdrawal and etoposide induce apoptosis in human lung carcinoma cell line a549 via distinct pathways. *Apoptosis* 2(2):199–206, 1997.
[54]Yogalingam, G., and A. M. Pendergast. Abl kinases regulate autophagy by promoting the trafficking and function of lysosomal components. *J. Biol. Chem.* 283(51):35941–35953, 2008.